2-2003

The Proliferation Gene Expression Signature is a Quantitative Integrator of Oncogenic Events that Predicts Survival in Mantle Cell Lymphoma

Andreas Rosenwald
1The Lymphoma/Leukemia Molecular Profiling Project

George Wright
National Cancer Institute, NIH, Bethesda, Maryland

Adrian Wiestner
National Cancer Institute, NIH, Bethesda, Maryland

Wing Chan
1The Lymphoma/Leukemia Molecular Profiling Project

Joseph Connors
1The Lymphoma/Leukemia Molecular Profiling Project

See next page for additional authors

Authors

Andreas Rosenwald, George Wright, Adrian Wiestner, Wing Chan, Joseph Connors, Elias Campo, Randy Gascoyne, Thomas Grogan, Konrad Muller-Hermelink, Erlend B. Smeland, Michael Chiorazzi, Jena M. Giltnane, Elaine M. Hurt, Hong Zhao, Lauren Averett, Sarah Henrickson, Liming Yang, John Powell, Wyndham H. Wilson, Elaine S. Jaffe, Richard Simon, Richard D. Klausner, Emilio Montserrat, Francesc Bosch, Timothy Greiner, Dennis D. Weisenburger, Warren G. Sanger, Bhavana J. Dave, James C. Lynch, Julie Vose, James O. Armitage, Richard I. Fisher, Thomas P. Miller, Michael LeBlanc, German Ott, Stein Kvaloy, Harald Holte, Jan Delabie, and Louis M. Staudt

The proliferation gene expression signature is a quantitative integrator of oncogenic events that predicts survival in mantle cell lymphoma

Andreas Rosenwald,[1, 2] George Wright,[1, 5] Adrian Wiestner,[1, 2] Wing C. Chan,[1, 9]
Joseph M. Connors,[1, 18] Elias Campo,[1, 8] Randy D. Gascoyne,[1, 18] Thomas M. Grogan,[1, 13, 17]
H. Konrad Muller-Hermelink,[1, 19] Erlend B. Smeland,[1, 22] Michael Chiorazzi,[1, 2] Jena M. Giltnane,[1, 2]
Elaine M. Hurt,[1, 2] Hong Zhao,[1, 2] Lauren Averett,[1, 2] Sarah Henrickson,[1, 2] Liming Yang,[1, 7] John Powell,[1, 7]
Wyndham H. Wilson,[1, 3] Elaine S. Jaffe,[1, 4] Richard Simon,[1, 5] Richard D. Klausner,[1, 6] Emilio Montserrat,[1, 8]
Francesc Bosch,[1, 8] Timothy C. Greiner,[1, 9] Dennis D. Weisenburger,[1, 9] Warren G. Sanger,[1, 10]
Bhavana J. Dave,[1, 9] James C. Lynch,[1, 11] Julie Vose,[1, 12] James O. Armitage,[1, 12] Richard I. Fisher,[1, 16, 17]
Thomas P. Miller,[1, 14, 17] Michael LeBlanc,[1, 15, 17] German Ott,[1, 19] Stein Kvaloy,[1, 20] Harald Holte,[1, 20]
Jan Delabie,[1, 21] and Louis M. Staudt[1, 2,*]

[1] The Lymphoma/Leukemia Molecular Profiling Project
[2] Metabolism Branch, [3] Medicine Branch, [4] Laboratory of Pathology
Center for Cancer Research, National Cancer Institute, NIH, Bethesda, Maryland
[5] Biometric Research Branch, Division of Cancer Treatment and Diagnosis
[6] Center for Cancer Research
National Cancer Institute, NIH, Bethesda, Maryland
[7] Bioinformatics and Molecular Analysis Section, CBEL, CIT, NIH, Bethesda, Maryland
[8] Hospital Clinic, University of Barcelona, Barcelona, Spain
[9] Department of Pathology and Microbiology, [10] Department of Pediatrics, [11] Department of Preventive and
Societal Medicine, [12] Department of Internal Medicine
University of Nebraska Medical Center, Omaha, Nebraska
[13] Department of Pathology, [14] Department of Medicine
University of Arizona Cancer Center, Tucson, Arizona
[15] Fred Hutchinson Cancer Research Center, Seattle, Washington
[16] James P. Wilmot Cancer Center, University of Rochester School of Medicine, Rochester, New York
[17] Southwest Oncology Group
[18] British Columbia Cancer Center, Vancouver, British Columbia, Canada
[19] Department of Pathology, University of Würzburg, Würzburg, Germany
[20] Department of Oncology, [21] Department of Pathology, [22] Department of Immunology
The Norwegian Radium Hospital, Oslo, Norway
*Correspondence: lstaudt@mail.nih.gov

Summary

We used gene expression profiling to establish a molecular diagnosis of mantle cell lymphoma (MCL), to elucidate its pathogenesis, and to predict the length of survival of these patients. An MCL gene expression signature defined a large subset of MCLs that expressed cyclin D1 and a novel subset that lacked cyclin D1 expression. A precise measurement of tumor cell proliferation, provided by the expression of proliferation signature genes, identified patient subsets that differed by more than 5 years in median survival. Differences in cyclin D1 mRNA abundance synergized with INK4a/ARF locus deletions to dictate tumor proliferation rate and survival. We propose a quantitative model of the aberrant cell cycle regulation in MCL that provides a rationale for the design of cell cycle inhibitor therapy in this malignancy.

S I G N I F I C A N C E

From a mechanistic standpoint, our results demonstrate that mathematical models can reveal the synergism between oncogenic events in a human cancer. The proliferation gene expression signature functioned as a quantitative integrator of multiple oncogenic aberrations. As such, the proliferation signature was better at predicting length of survival than were other models based on the individual oncogenic events. From a clinical standpoint, our gene expression-based model of survival provides the most precise prognostic index yet described for MCL. Our survival model suggests that therapeutic modulation of the cell cycle has the potential to significantly prolong the life of these patients.

Introduction

Mantle cell lymphoma (MCL) was originally identified as a morphologically distinct subtype of non-Hodgkin's lymphoma, and subsequently the t(11;14) translocation was defined as a characteristic molecular feature of this lymphoma subtype (Campo et al., 1999; Raffeld and Jaffe, 1991; Swerdlow and Williams, 2002; Weisenburger and Armitage, 1996). This translocation leads to overexpression of cyclin D1, a D-type cyclin that is not usually expressed at high levels in normal B lymphocytes (Rosenberg et al., 1991). Current WHO guidelines for the diagnosis of MCL rely on morphological assessment supplemented with analysis of cyclin D1 translocation or overexpression (Jaffe et al., 1999). Cyclin D1 translocation and expression has been helpful in distinguishing MCL from other chronic B cell malignancies, such as small lymphocytic lymphoma/chronic lymphocytic leukemia (SLL/CLL), follicular lymphoma, and marginal zone lymphoma. Nevertheless, some lymphomas that lack cyclin D1 expression are morphologically similar to MCL and may be variant forms of this lymphoma type (Yatabe et al., 2000).

MCL accounts for 6% of all non-Hodgkin's lymphomas and a higher fraction of deaths from lymphoma, given that it is an incurable malignancy (Campo et al., 1999; Swerdlow and Williams, 2002; TNHLCP, 1997). The length of survival of MCL patients following diagnosis is quite variable. The median survival in MCL is approximately 3 years, but some patients have an aggressive disease to which they succumb in less than 1 year. Other patients have a comparatively indolent disease, and some patients may survive more than 10 years.

Faced with this clinical heterogeneity, many attempts have been made to develop prognostic markers of survival. Several morphological subtypes of MCL have been recognized, and a blastic variant of MCL has been associated with short survival in several studies (Argatoff et al., 1997; Bosch et al., 1998; Lardelli et al., 1990). High tumor cell proliferation has also been associated with shorter survival (Argatoff et al., 1997; Bosch et al., 1998; Raty et al., 2002; Velders et al., 1996), as has INK4a/ARF locus deletion (Dreyling et al., 1997; Pinyol et al., 1998) and p53 mutation or protein overexpression (Greiner et al., 1996; Hernandez et al., 1996; Louie et al., 1995). However, the prognostic groups defined by each of these markers were still clinically heterogeneous, demonstrating that each marker alone does not fully account for the clinical behavior of these tumors.

In the present study, our first goal was to establish a molecular diagnosis of MCL based on gene expression that could reliably distinguish this disease from other lymphoma types. With such a diagnostic test in hand, we investigated which genes had expression patterns that correlated with length of survival. We show that genes involved in proliferation have an overriding influence on the clinical course and can be used to construct a powerful predictor of survival. Additionally, we demonstrate that the proliferation signature integrates several oncogenic mechanisms in MCL that govern the cell cycle, leading us to propose a quantitative model for MCL pathogenesis.

Results

Molecular diagnosis of MCL

To establish a molecular diagnosis of MCL based on gene expression, we began by identifying lymphoma cases that were morphologically consistent with this diagnosis upon pathologi-

cal review. Since the t(11;14) translocation and cyclin D1 overexpression have been consistently associated with MCL, we measured cyclin D1 mRNA levels in each potential MCL case by quantitative RT-PCR. Of the 101 cases with MCL histology, 92 expressed cyclin D1 mRNA, and these were considered the "core" group of bona fide MCLs. We used Lymphochip DNA microarrays (Alizadeh et al., 1999) to profile gene expression in all 101 lymphoma cases with MCL morphology. For comparison, we profiled gene expression in 20 cases of SLL and used previously published gene expression data from two subgroups of diffuse large B cell lymphoma (DLBCL), germinal center B cell-like (GCB) DLBCL (134 cases), and activated B cell-like (ABC) DLBCL (83 cases) (Rosenwald et al., 2002). Several thousand genes were differentially expressed between MCL and the other lymphoma subtypes with high statistical significance (p < 0.001), and those "MCL signature genes" that were most highly and differentially expressed in MCL are shown in Figure 1A (a complete listing of these genes is available at http://llmpp.nih.gov/MCL).

To create a gene expression-based diagnostic test for MCL, we developed a Bayesian statistical method that was able to distinguish MCL from other lymphoma subtypes. In brief, we began by identifying the most differentially expressed genes between cyclin D1-positive MCL and each of the other lymphoma types. These differentially expressed genes were combined to form a series of binary predictors that estimated the probability that a particular lymphoma sample was MCL or one of the other lymphoma types. We used a cutoff of 90% probability in assigning a sample to a lymphoma type based on these binary predictors.

To insure the reproducibility of our method, we divided the cyclin D1-positive MCL cases into two equal groups: a "training set" that was used to develop the MCL diagnostic test, and a "validation set" that was used to evaluate the test. We optimized the number of genes in each binary lymphoma type predictor so as to minimize the number of classification errors when the predictor was applied to the training set cases in a crossvalidation, leave-one-out fashion. We deliberately excluded cyclin D1 as a lymphoma type distinction gene because we wished to apply our model to potential MCL cases that were cyclin D1-negative. Using the optimized lymphoma type predictors, 100% of the training set cases were correctly classified (Figure 1B). When applied to the validation set, the model correctly classified 98% of the cyclin D1-positive MCL cases as MCL, thus establishing this method as a reliable MCL diagnostic test (Figure 1B).

We applied this MCL diagnostic test to 9 lymphoma cases that were morphologically consistent with MCL but were negative for cyclin D1 expression by quantitative RT-PCR analysis. Seven were classified as MCL, one was classified as GCB DLBCL, and one was not assigned to any lymphoma group based on the probability cutoff used. As shown in Figure 1C, the 7 cyclin D1-negative MCL tumors were comparable to cyclin D1-positive MCL tumors with respect to expression of 42 MCL signature genes. Interestingly, 2 of these cyclin D1-negative tumors expressed higher levels of cyclin D3, and 1 expressed higher levels of cyclin D2 than were detected in cyclin D1-positive MCLs. At present, the molecular mechanisms underlying the expression of other D-type cyclins in these cases are unclear, but this finding suggests that these tumors may have found alternative ways to increase cell cycle progression in the absence of cyclin D1. Overall survival of patients with cyclin

D1-positive MCL was not statistically different from that of patients with cyclin D1-negative MCL (Figure 1D).

A gene expression-based predictor of survival

We next used gene expression to develop a predictor of length of survival following diagnosis of MCL. The median survival of the patients with cyclin D1-positive MCL was 2.8 years, but the lengths of survival were quite heterogeneous (Figure 1D). Many patients died within the first 2 years following diagnosis, yet 15% (14/92) of the patients survived more than 5 years and 3 patients survived more than 10 years. It is important to emphasize that the diagnosis of MCL in these patients was based on morphology, cyclin D1 expression, and expression of genes that distinguish MCL from other non-Hodgkin's lymphomas. Thus, the differences in survival among these patients are unlikely to be due to the inadvertent inclusion of other lymphoma types in our cohort.

We used a supervised approach to discover "survival prediction" genes with expression patterns that were associated with length of survival among MCL patients in the training sets. The expression levels of 48 genes correlated with survival with high statistical significance ($p < 0.001$), and all of these were more highly expressed in tumors from patients with short survival. As in our previous analysis of survival of patients with DLBCL (Rosenwald et al., 2002), we functionally classified the survival prediction genes based on their membership in gene expression "signatures." A gene expression signature is a group of genes that are coordinately expressed in association with a particular biological process (Shaffer et al., 2001). Notably, 58% of the survival prediction genes (28/48) belonged to the proliferation gene expression signature. This signature is composed of genes that are expressed at higher levels in dividing cells than in quiescent cells, including genes required for DNA replication, cell cycle progression, and the metabolic demands of proliferation (Shaffer et al., 2001). We further focused our attention on those survival prediction genes that were most variably expressed among the MCLs (i.e., in the top third of gene expression variance) in order to facilitate the subsequent analysis of these genes by other methodologies; 34 genes satisfied this selection criterion, of which 20 belonged to the proliferation signature. We averaged the expression levels of these 20 genes to create a proliferation signature average for each MCL case. Tumor cell proliferation rate can also be estimated by the number of Ki67-positive cells or by the mitotic index, and these data were available on 14 patients. As expected, the proliferation signature average was correlated with the number of Ki67-positive cells ($r = 0.69$) and the mitotic index ($r = 0.62$).

Within the training set, the proliferation signature average was inversely correlated with survival with high statistical significance (1.92×10^{-5}). Importantly, the proliferation signature average also predicted survival of patients in the validation set with high significance (7.44×10^{-5}), thus demonstrating the reproducibility of this gene expression-based predictor. When all cases were considered together, this predictor correlated with survival with a significance of $p = 5.07 \times 10^{-9}$. None of the other survival prediction genes from the original set of 48 improved the prognostic ability of the proliferation signature average in multivariate models. Of note, we could also construct a model from only 4 proliferation signature genes (CDC2, ASPM, tubulin α, CENP-F) that predicted length of survival with high statistical significance on the total set of cases ($p = 2.67 \times 10^{-8}$).

To visualize the predictive power of our survival model, we ranked the patients according to the expression of the proliferation signature genes in their tumors, and divided them into 4 equal quartiles. Figure 2B shows Kaplan-Meier plots of overall survival of patients in each of these quartiles, within the training set, the validation set, and the total set of cases. These plots indicate that the proliferation signature can identify patient subsets with strikingly different survival times. The median survival times of patients in the four quartiles were: 6.71 years (quartile 1), 3.28 years (quartile 2), 2.31 years (quartile 3), and 0.83 years (quartile 4). It is important to emphasize that the quartile method that we used to group MCL patients is merely a way of illustrating the quantitative relationship between proliferation and survival. The proliferation signature average is a continuous variable that assigns, for each patient, a discrete probability of survival at every time point following diagnosis. The proliferation signature average varied over a 13.5-fold range and a 2-fold increase in the proliferation signature average corresponded to a 3.6-fold increased relative risk of dying.
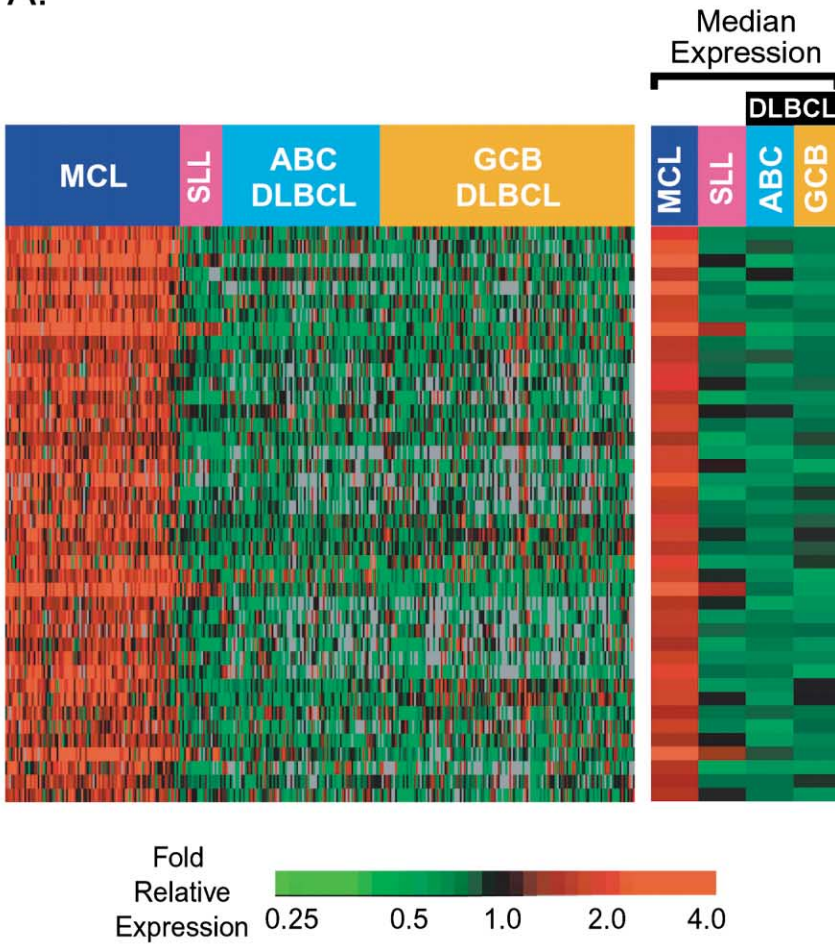
Several histological subtypes of MCL can be discerned, and these have been shown to differ with respect to proliferation rate and survival (Argatoff et al., 1997; Bosch et al., 1998). We subdivided our MCL cases by morphology into classical (68.4%), blastic (9.8%), pleomorphic (6.5%), and small cell (9.8%) subtypes. As expected, the cases with blastic morphology had the highest expression of the proliferation signature (Figure 3A) and the shortest survival (Figure 3B). However, the morphological categorization of MCL was a much weaker predictor of survival ($p = 5.7 \times 10^{-3}$) than was the proliferation signature.

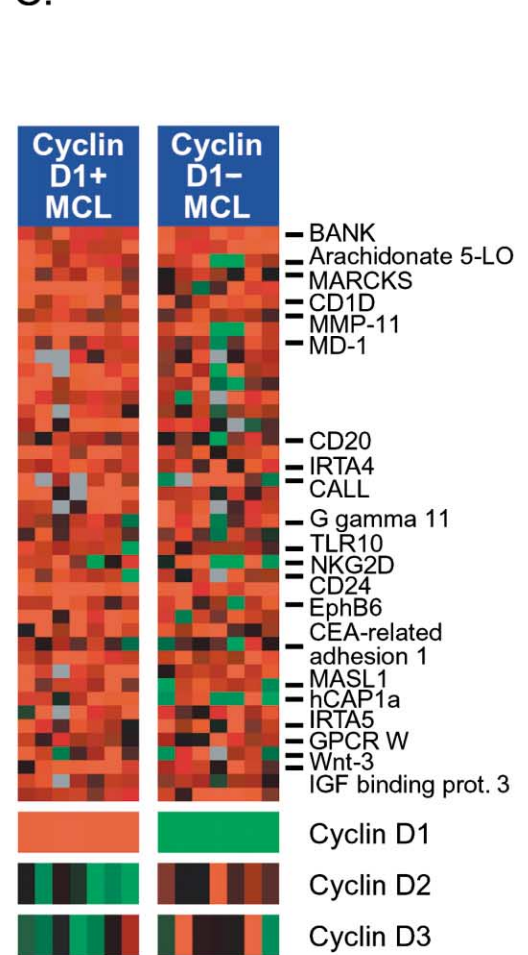## The proliferation signature integrates oncogenic events associated with survival

Having related the proliferation signature to overall survival in MCL, we searched for molecular mechanisms that might explain the variable proliferation of MCLs. We noted that the mRNA expression of the cyclin D1 coding region, as measured by a quantitative RT-PCR assay, was higher in more proliferative MCLs ($p = 1.4 \times 10^{-4}$; Figure 4A). Further, the abundance of cyclin D1 coding region mRNA was a univariate predictor of survival ($p = 4.69 \times 10^{-4}$), but was not as strong a prognostic marker as the proliferation signature (Figure 4E). The expression of cyclin D1 coding region mRNA was correlated with proliferation ($p = 1.4 \times 10^{-4}$), and therefore did not add to the prognostic strength of the proliferation signature in a 2-component model. These results suggests a direct relationship between cyclin D1 expression levels and proliferation rate in MCL, and demonstrate that the length of survival of MCL patients depends upon quantitative differences in progression from G1 to S phase of the cell cycle.

MCLs can express various cyclin D1 mRNA isoforms that all include the cyclin D1 coding region but that differ in the length of their 3′ untranslated regions (UTRs) (Figure 4G). The 4.5 kb mRNA isoform has an extended UTR that includes an AT-rich segment with the potential to decrease mRNA stability (Lebwohl et al., 1994; Lin et al., 2000; Rimokh et al., 1994). Some MCLs have alterations in the cyclin D1 genomic sequences that encode the 3′ UTR region, and these cases do not express the 4.5 kb mRNA isoform, but instead express a 1.7 kb mRNA isoform or other short mRNAs that lack the potential mRNA destabilizing element in the 3′ UTR (Bosch et al., 1994; de Boer
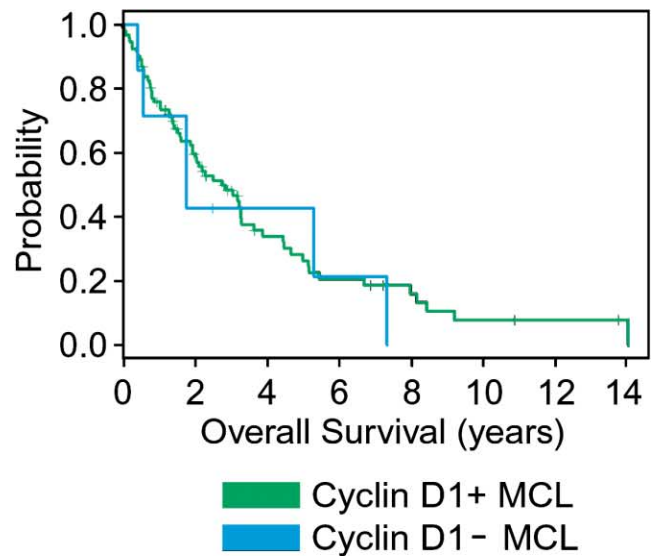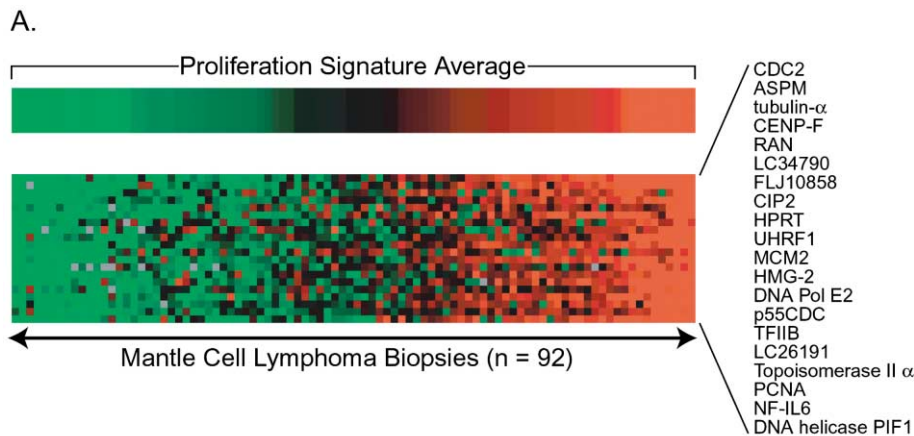
A.

C.

B.

D.

A.

B.

et al., 1995; Rimokh et al., 1994; Seto et al., 1992; Withers et al., 1991). On the Lymphochip DNA microarray, the cyclin D1 features correspond to the extended 3′ UTR, and therefore can only detect expression of the 4.5 kb mRNA. In contrast, the quantitative RT-PCR assay for the cyclin D1 coding region can detect shorter isoforms lacking the extended 3′ UTR as well as the 4.5 kb isoform.

With some MCL samples, we obtained little if any signal from the cyclin D1 3′ UTR features on the microarray, yet these same samples had abundant expression of the cyclin D1 coding region as assessed by the quantitative RT-PCR assay (Figure 4A). This pattern suggests that these MCL tumors preferentially express the short cyclin D1 mRNA isoforms lacking the extended 3′ UTR. Notably, the MCLs with this expression pattern

Figure 1. Molecular diagnosis of mantle cell lymphoma

A: Hierarchical clustering of expression measurements from 42 MCL signature genes that are more highly expressed in 92 MCL samples than in 20 SLL, 83 ABC LBCL, and 134 GCB DLBCL samples (see text for details). Each column represents a single lymphoma specimen, and each row represents expression of a single gene. Red squares indicate increased expression and green squares indicate decreased expression relative to the median expression level according to the color scale shown. The right panel shows the median gene expression for the 42 MCL signature genes in each of the lymphoma subgroups.
B: Performance of the gene expression-based diagnostic test for MCL in each of the three models (MCL versus ABC DLBCL, MCL versus GCB DLBCL, and MCL versus SLL) in the "training set" and in the "validation set" of cases.
C: Expression of MCL signature genes in seven cyclin D1-positive and seven cyclin D1-negative lymphoma cases. Cyclin D1-negative cases had MCL morphology and immunophenotype and were classified as MCL based on their gene expression profile. Shown below is the relative gene expression of cyclin D1 (as measured by quantitative RT-PCR) and cyclins D2 and D3 (as measured by DNA microarray analysis).
D: Kaplan-Meier estimates of overall survival of patients with cyclin D1-positive and cyclin D1-negative MCL.
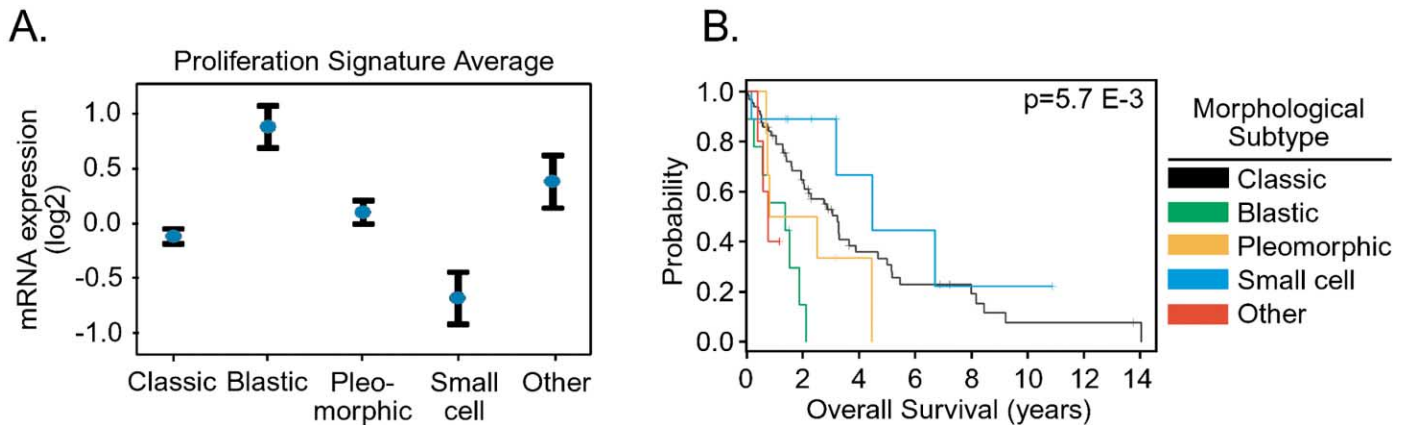
Figure 3. Proliferation and survival rates in different histological subtypes of MCL

A: Proliferation signature averages in the classic, blastic, pleomorphic, and small cell subtypes of MCL. The dots represent the mean value within each class, and the bars represent the standard error of that mean estimate.
B: Kaplan-Meier plots of overall survival of patients in different histological MCL subtypes.

were generally among those with high proliferation (Figure 4A). Based on levels of cyclin D1 3′ UTR expression, we defined a "3′ UTR low" group of 17 MCL cases and a "3′ UTR high" group of 75 MCL cases (Figure 4B). The 3′ UTR low group had a 1.58-fold higher level of cyclin D1 coding region mRNA than did the 3′ UTR high group (p = 5.4×10^{-5}), thus providing one potential molecular mechanism for the variable expression of cyclin D1 coding region mRNAs (Figure 4C). Further, the 3′ UTR low group had a 1.83-fold higher expression of the proliferation signature (p = 1.3×10^{-7}; Figure 4D) and a shorter survival than the 3′ UTR high group (p = 7.97×10^{-5}; Figure 4F).

We next investigated whether deletions of tumor suppressor genes were associated with proliferation rate and survival in MCL. We used a quantitative PCR assay to detect genomic loss of one or both alleles of the INK4a/ARF locus, which encodes two tumor suppressors, p16^{INK4a} and p14^{ARF}. INK4a/ARF locus deletions were detected in 21% (18/85) of the cases and were preferentially observed among the more proliferative MCLs (Figure 5A). The INK4a/ARF locus can also be transcriptionally silenced by the polycomb family protein BMI-1 (Jacobs et al., 1999), and BMI-1 is amplified and/or overexpressed in some MCLs (Bea et al., 2001). Notably, BMI-1 was overexpressed in some highly proliferative MCLs that lacked INK4a/ARF locus deletion (Figure 5A).

We next tested whether the proliferation rate of MCL tumors could be modeled using a combination of the INK4a/ARF locus deletional status and the expression of cyclin D1 coding region mRNA. Both of these parameters added independently to a model of survival: cyclin D1 coding region expression added to the significance of a model based on INK4a/ARF locus deletion alone (p = 2.6×10^{-3}), and INK4a/ARF locus deletion added to the significance of a model based on cyclin D1 coding region expression alone (p = 3.6×10^{-5}). This finding suggests that increased cyclin D1 expression and INK4a/ARF locus deletion cooperate mechanistically to increase the proliferation rate (see Discussion). INK4a/ARF locus deletions were also associated with shorter survival (p = 4.88×10^{-4}; Figure 5B). Again, INK4a/ARF locus deletional status and cyclin D1 coding region expression added independent predictive power to a combined statis-

tical model of survival, such that the combined model had a greater significance (p = 3.59×10^{-6}) than models of survival based on either of these components alone (Figure 5C).

Deletional events at the p53 and ATM loci had distinct but overlapping distributions with respect to each other and with respect to INK4a/ARF locus deletions (Figure 5A). p53 deletions were found in 9 MCL cases (11%), and concurrent deletions of INK4a/ARF locus and ATM were found in 3 and 6 cases, respectively. ATM deletions were more frequent among the MCLs, occurring in 30 cases (35%), and were concurrent with INK4a/ARF locus and p53 deletions in 8 and 6 cases, respectively. These findings suggest that loss of these tumor suppressor genes provided nonredundant selective advantages to the MCLs during the natural histories of these lymphomas. p53 deletions were not strongly associated with proliferation (Figure 5A) or survival (p = 0.25; data not shown), although the number of p53 deletional events in our series was small, and some MCL cases may have mutations of p53 without deletion. ATM deletions were present in tumors with both low and high proliferation rates (Figure 5A), and had no apparent relationship to survival (p = 0.66; data not shown).

Discussion

We have taken a quantitative approach to understand the pathogenesis of MCL and to account for the variable survival of these patients. By precisely measuring the expression of genes associated with proliferation, we found that the degree of tumor cell proliferation provides a powerful predictor of survival for this lymphoma. Further, our approach provides a quantitative rather than qualitative framework for the molecular pathogenesis of this disease, in which higher cyclin D1 mRNA levels are reflected in higher tumor cell proliferation and shorter survival.

The defining oncogenic event in most MCLs is translocation and overexpression of cyclin D1, and this shared pathogenetic feature was central to the success of our quantitative approach. Using an RT-PCR assay, we defined a cohort of patients whose tumors expressed cyclin D1 and found that they also expressed a set of MCL signature genes that distinguished this lymphoma
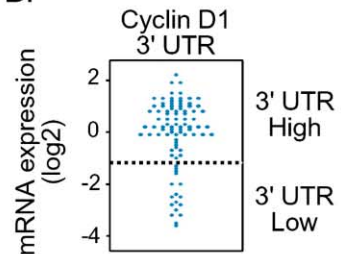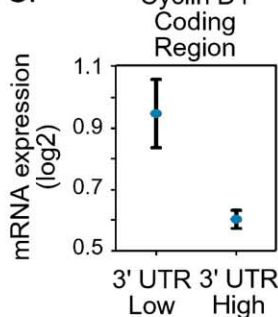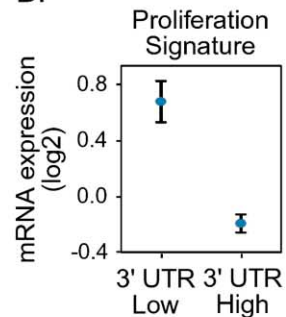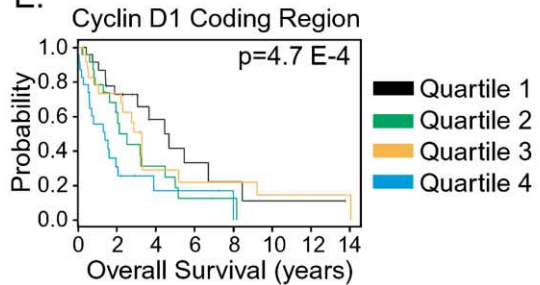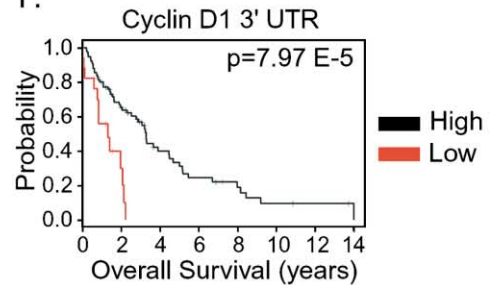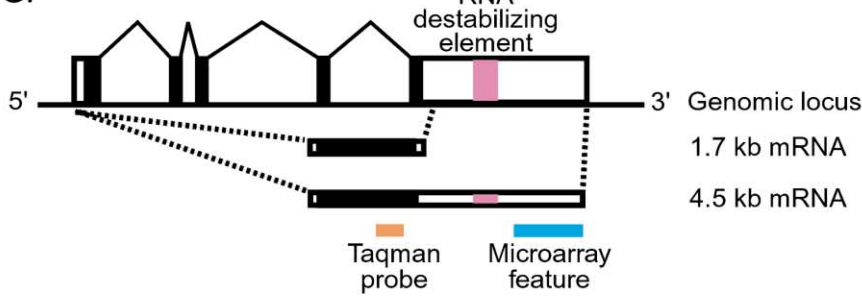
Figure 4. Relationship between cyclin D1 expression, proliferation, and survival in MCL

A: Relative cyclin D1 mRNA expression of the coding region (measured by quantitative RT-PCR, upper panel) and of the 3' UTR (measured by DNA microarray analysis). The 92 cyclin D1-positive MCL cases are ordered according to their proliferation signature average (lower panel). The cyclin D1 expression is depicted over a 9-fold range, whereas the proliferation signature expression is depicted over a 4-fold range.

B: Histogram of cyclin D1 3' UTR levels. Shown is a cutpoint that divides the MCL cases into a "3' UTR low" group (17 cases) and a "3' UTR high" group (75 cases).

C: Level of cyclin D1 coding region mRNA in the "3' UTR low" and "3' UTR high" groups of MCL. The dots represent the mean value within each class, and the bars represent the standard error of that mean estimate.

D: Proliferation signature averages of MCL cases in the "3' UTR low" and "3' UTR high" groups of MCL. The dots represent the mean value within each class, and the bars represent the standard error of that mean estimate.

E: Kaplan-Meier estimates of overall survival according to the level of cyclin D1 coding region mRNA expression.

F: Kaplan-Meier plot of overall survival according to cyclin D1 3'UTR expression.

G: The cyclin D1 locus: alternative 3' polyadenylation sites can result in the expression of a short (1.7 kb) and a long (4.5 kb) cyclin D1 mRNA.
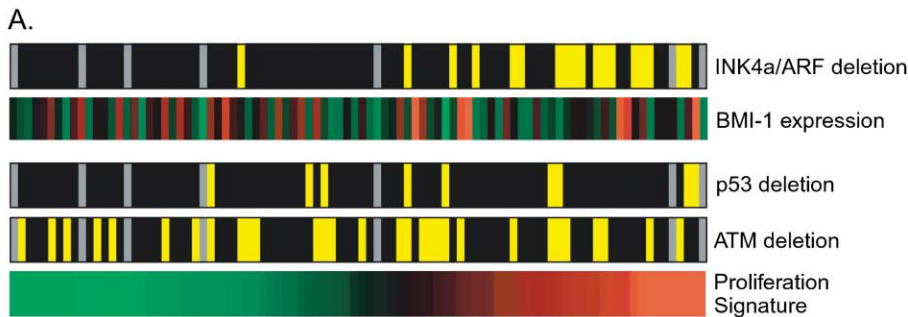
Figure 5. Deletions of INK4a/ARF, ATM, and p53 loci in MCL

A: Genomic loss of one or both alleles of the INK4a/ARF, ATM, and p53 loci as measured by quantitative PCR. MCL cases are ordered by their proliferation signature averages, and deletions are indicated by yellow squares. Black squares indicate wild-type configuration of the genomic loci, and gray squares indicate missing data. BMI-1 expression is depicted over a 9-fold range.

B: Influence of INK4a/ARF locus deletion on overall survival.
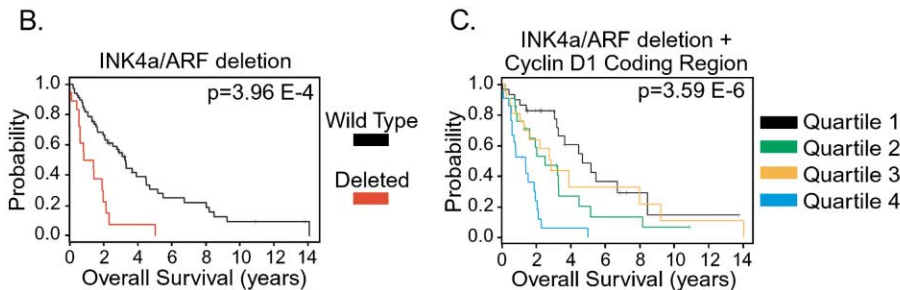
type from others. By basing our molecular diagnosis on the expression of cyclin D1 and the MCL signature genes, we could be confident that we were studying patients with highly related cancers, which is critical when searching for the molecular determinants of survival.

The MCL gene expression signature further allowed us to identify a new subtype of MCL that is cyclin D1-negative. The existence of cyclin D1-negative MCL has been controversial, since other methods of detecting cyclin D1 translocations or expression vary in sensitivity, and since other lymphoid malignancies can express cyclin D1. We identified a group of lymphomas that were not only morphologically indistinguishable from cyclin D1-positive MCLs, but also shared expression of MCL signature genes. These patients with cyclin D1-negative MCL did not differ significantly in survival from patients with cyclin D1-positive MCL. Interestingly, some of the cyclin D1-negative MCLs expressed either cyclin D2 or D3, suggesting that these cyclins can functionally substitute for cyclin D1 in MCL. At present, we do not know whether the expression of the other D-type cyclins in these cases is due to genomic rearrangements of these genes or to increased transcription. Given the importance of the G1/S phase transition in MCL, it is highly likely that all of the cyclin D1-negative MCL tumors have acquired some mechanism to accelerate entry into S phase.

Among patients with cyclin D1-positive MCL, the proliferation signature was the sole gene expression feature that was significantly associated with survival. Using the proliferation signature average as a metric, we identified one quartile of MCL patients who had a median survival of 6.7 years, which is exceptionally long for this incurable malignancy. At the other end of the spectrum, we identified a quartile of patients who had particularly aggressive tumors and a median survival of only 0.8 years. This 5.9-year difference in survival highlights the potential value of the proliferation gene expression signature as a prognostic test in MCL. By contrast, previous analyses of tumor cell

proliferation in MCL relied on semiquantitative methods such as the mitotic index or immunohistochemical staining for Ki67 to define patient groups that differed in survival by only 2.1–2.7 years (Argatoff et al., 1997; Bosch et al., 1998; Raty et al., 2002; Velders et al., 1996).

Since our quantitative method accounts more fully for the varying survival of MCL patients, it could prove useful in the clinical management of these patients. Since the proliferation signature can be faithfully represented by as few as 4 genes, a limited set of quantitative RT-PCR assays could be used to assess tumor proliferation rate. In particular, we suggest that clinical trials in MCL should incorporate a quantitative measure of tumor proliferation rate. This would enable a direct comparison of the patients enrolled in different clinical trials and would provide a rational basis by which to compare trial results.

Various intensified treatments are being evaluated in MCL, including autologous and allogeneic bone marrow transplantation, modified chemotherapeutic regimens, and radioimmunotherapy (Barista et al., 2001; Gopal et al., 2002; Leonard et al., 2001). Our results suggest that it may be beneficial to stratify patients for entry into clinical trials of these regimens according to the expression of proliferation signature genes in their tumors. Clinical trials of intensified regimens might be designed to enroll only those patients whose tumor proliferation rate predicts an exceedingly short survival. Intensified regimens may not be appropriate for patients whose tumor proliferation rate predicts a longer survival, since these regimens may not prolong the survival of these patients and may unnecessarily expose them to treatment-related toxicities. Rather, these patients could be managed conservatively, with relatively nontoxic therapies given only as clinically indicated.

In addition to its value in prognosis, the proliferation signature proved very useful in establishing a quantitative model of MCL pathogenesis. In particular, the proliferation signature quantitatively integrated the effects of cyclin D1 expression and

deletion of the INK4a/ARF locus. However, our statistical model based on cyclin D1 expression and INK4a/ARF deletions accounted for only 32% of the variation in the proliferation signature average (data not shown), and therefore the proliferation signature may also reflect additional oncogenic events that are as yet unknown.

Higher expression of cyclin D1 mRNA was correlated with increased proliferation and decreased survival time. The importance of this oncogenic mechanism in MCL has been overlooked since previous studies have used only semiquantitative methods to assess cyclin D1 expression and tumor proliferation. We noted that many of the highly proliferative MCL tumors expressed mRNA species that contained the cyclin D1 coding region but not the extended 3′ UTR region, and this was associated with higher levels of cyclin D1 coding region expression. MCLs and other cancers have been shown to variably express cyclin D1 mRNA isoforms that differ in the length of their 3′ UTRs. The extended 3′ UTR of the 4.5 kb cyclin D1 isoform contains AT-rich sequences that can modulate the stability of the mRNA, and short cyclin D1 mRNA isoforms lacking this region are more stable (Lebwohl et al., 1994; Lin et al., 2000; Rimokh et al., 1994). In some MCLs, the genomic region corresponding to the extended 3′ UTR is deleted or rearranged, and these cases lack expression of the 4.5 kb mRNA isoform (de Boer et al., 1995; Rimokh et al., 1994; Seto et al., 1992; Withers et al., 1991). However, in some cells, the 4.5 and 1.7 kb isoforms coexist, and their relative abundance may be regulated by alternative polyadenylation and cleavage (Xiong et al., 1991). Regardless of the mechanism, our data demonstrate that selective expression of short cyclin D1 mRNA isoforms is a pathogenetic mechanism that is associated with increased cyclin D1 expression, more rapid proliferation, and shorter survival.

The relationship between increased cyclin D1 expression and increased proliferation suggests a quantitative model for the G1/S phase transition. In this model, an increase in the intracellular concentration of cyclin D1 promotes its assembly into active kinase complexes with cdk4 and cdk6 (cyclin D1/cdk4[6]), which would enhance the frequency at which the cell enters S phase by two mechanisms (reviewed in Sherr and McCormick, 2002). Cyclin D1/cdk4(6) kinases phosphorylate the retinoblastoma (Rb) gene product and thereby promote the release of E2F transcription factors that are required in S phase. Further, cyclin D1/cdk4(6) complexes interact with the cyclin-dependent kinase inhibitors p21 and p27kip1 and titrate these factors away from cyclin E/cdk2 kinase complexes. Whereas p21 and p27kip1 are potent inhibitors of cyclinE/cdk2, they fail to inhibit cyclin D1/cdk4(6). Increased cyclin E/cdk2 kinase activity promotes S phase entry by phosphorylating Rb and can sustain cell cycle progression by phosphorylating p27kip1, leading to its degradation in the proteosome. In keeping with this model, most p27kip1 in MCL cells is biochemically associated with cyclin D1 (Quintanilla-Martinez et al., 2003).

Our findings highlight the quantitative sensitivity of the G1/S phase transition to changes in D-type cyclin concentration. This cell cycle transition appears to behave like a rheostat regulated by cyclin D1 kinase complex levels rather than an on/off switch that is activated when a threshold level of cyclin D1 is achieved (see Sherr and Roberts, 1995, 1999 for a complete discussion). In this model, the fraction of cells in the tumor clone that are in G1 phase, and consequently the tumor proliferation rate, would be influenced quantitatively by the abundance of cyclin

D1 kinase complexes. Our data demonstrate that small changes in the expression of D-type cyclins can have significant effects on tumor cell proliferation and the clinical course of cancer patients.

High expression of the proliferation signature in MCL was also associated with deletion of the INK4a/ARF locus. This locus encodes two structurally unrelated tumor suppressors, p16[INK4a] and p14[ARF] (Sherr and McCormick, 2002), and deletions of this genomic region in MCL typically inactivate both the p16[INK4a] and p14[ARF] genes and are frequently homozygous (Dreyling et al., 1997; Pinyol et al., 1997, 1998, 2000). Further, the p16[INK4a] gene does not sustain point mutations in MCLs as it does in melanoma and other cancers (Pinyol et al., 1997, 2000). Finally, we and others (Bea et al., 2001) observed overexpression of the BMI-1 gene in MCLs that lacked deletion of the INK4a/ARF locus, which is notable since BMI-1 represses transcription of both p16[INK4a] and p14[ARF] (Sherr and McCormick, 2002). These considerations suggest that the INK4a/ARF deletions in MCL may be selected to circumvent the actions of both p16[INK4a] and p14[ARF].

p16[INK4a] regulates the G1/S phase transition by forming binary complexes with cdk4 and cdk6, thereby preventing these subunits from associating with molecular chaperones that promote their association with D-type cyclins (reviewed in Sherr and McCormick, 2002). p16[INK4a] deletion and increased cyclin D1 expression may therefore promote the G1/S phase transition by the same mechanism. Nonetheless, our statistical models demonstrated that cyclin D1 expression and INK4a/ARF deletions cooperated to quantitatively increase proliferation and shorten survival. One model to account for this oncogenic synergism would propose that the presence of wild-type levels of p16[INK4a] blunts the effect of increased cyclin D1 expression by preventing cyclin D1 from forming active kinase complexes. Although many cancer types have disruption in only one component of the Rb pathway (Sherr and McCormick, 2002), our results suggest that some cancers may accumulate multiple oncogenic lesions that cooperate to quantitatively interfere with this pathway and promote proliferation.

Studies of mouse strains with selective disruption of the p14[ARF] gene demonstrate that p14[ARF] also regulates proliferation. p14[ARF]-deficient mouse embryo fibroblasts and pre-B cells divide more rapidly than their wild-type counterparts and fail to senesce during repeated passaging in vitro (Kamijo et al., 1998; Randle et al., 2001). Further, in transgenic mice overexpressing c-*myc*, p14[ARF]-deficiency accelerates lymphoma formation and the proliferation rate of the malignant B cells ex vivo (Eischen et al., 1999; Schmitt et al., 2002). Although the mechanisms underlying the enhanced proliferation of p14[ARF]-deficient cells are not completely understood, these observations suggest that loss of p14[ARF] may contribute to the enhanced proliferation of INK4a/ARF-deleted MCL tumors.

An important function of p14[ARF] is to augment p53 function by antagonizing MDM2 (Sherr and McCormick, 2002), and loss of this p14[ARF] function may contribute to the enhanced proliferation and shorter survival of MCL patients with INK4a/ARF deletions. p14[ARF] is induced by a variety of oncogenes that promote inappropriate proliferation, leading to a p53-dependent cell cycle arrest or apoptosis (Kamijo et al., 1997, 1998). In MCL tumors with wild-type INK4a/ARF loci, it is conceivable that some oncogenic stimuli may activate p14[ARF] and constrain proliferation. In this scenario, MCL tumor cells that sustain p14[ARF] deletions would have a selective advantage. Our observation that INK4a/

ARF locus deletions and cyclin D1 expression synergize to predict the proliferation signature may therefore reflect a cooperation between the p53 pathway and the RB pathway in controlling cell cycle progression. However, we found that some MCL tumors had deletions of both the INK4a/ARF and p53 loci, suggesting that p53 deletion may provide additional selective advantages, such as evasion of apoptosis.

Though many of the oncogenic events in MCL are designed to promote S phase entry, deletions of the ATM tumor suppressor gene appear to play a different role. Roughly one-third of the MCL tumors in our study had ATM deletions, irrespective of tumor proliferation rate, INK4a/ARF locus deletional status, and cyclin D1 expression and survival. This finding suggests that the tumor suppressor role of ATM in MCL is unrelated mechanistically to G1/S phase checkpoint. ATM is required for activation of p53 in response to DNA damage and abnormal telomeres, and during normal immunoglobulin V-D-J recombination (Karlseder et al., 1999; Kastan et al., 1992; Perkins et al., 2002). However, ATM deletions coincided with p53 deletions in several MCL cases, suggesting that loss of these genes may serve distinct functions in the pathogenesis of some MCLs.

Finally, our data provide quantitative insights into the potential of cell cycle inhibitors in the therapy of MCL. Although cell cycle inhibitors would not necessarily be curative in MCL, it is possible that they could alter its natural history, yielding a chronic lymphoproliferative disease that could be managed conservatively. Could, for example, a cell cycle inhibitor shift a patient's lymphoma from the last to the first quartile of the proliferation signature average, thereby prolonging the patient's survival by more than 5 years? An inhibitor targeting the basic cell cycle machinery would likely require careful dose titration in order to limit toxicity during chronic administration. Alternatively, it is possible that inhibitors that target the G1/S checkpoint by disrupting cyclin D1/cdk4(6) complexes could be administered chronically, and might turn MCL into a clinically manageable disease.

Experimental procedures

Patients

Tumor biopsies from 101 untreated patients with no history of a previous lymphoma were included in the present study, according to a protocol approved by the National Cancer Institute institutional review board. Tumor histology was reviewed by a panel of 8 hematopathologists, and 92 biopsy specimens were classified as mantle cell lymphoma, based on established morphologic and immunophenotypic criteria (Jaffe et al., 2001). All of these 92 cases showed overexpression of cyclin D1 mRNA by a quantitative RT-PCR assay and, in most cases, immunohistochemistry demonstrated overexpression of cyclin D1 also on the protein level. In the remaining nine lymphoma specimens, the morphology and immunophenotype of the tumor cells were consistent with the diagnosis of MCL, but there was no evidence of the t(11;14) translocation or cyclin D1 protein expression. All nine of these cases were negative for cyclin D1 mRNA expression by quantitative RT-PCR. Only data obtained from the 92 patients with cyclin D1-positive MCL were used to create the gene expression-based predictor of survival. Among these 92 patients, 72 were male and 19 female (no information was available on one patient), the median age at diagnosis was 61.5 years (range 38 to 92.5 years) and median survival was 2.8 years. 84 patients received multiagent chemotherapy as needed symptomatically, 6 received no treatment, and no information on treatment was available in 2 patients.

Microarray procedures

Lymphochip DNA microarrays (Alizadeh et al., 1999) containing 12,196 cDNA elements were used to quantitate mRNA expression in the lymphoma samples, as described previously (Rosenwald et al., 2002). The complete gene expression data set is available at http://llmpp.nih.gov/MCL.

Real-time quantitative PCR

To measure cyclin D1 mRNA expression by real-time quantitative RT-PCR, an aliquot of the mRNA used for the microarray experiments was diluted to approximately 0.5 ng/μl. 5 μl of the diluted mRNA were used for each RT-PCR reaction using TaqMan™ reagents and analyzed on an Applied Biosystems Thermal Cycler. All samples were run in triplicate, and a probe for the β2-microglobulin gene was chosen as a reference. Primers and Taqman probes for both β2-microglobulin and the coding region of cyclin D1 have been described previously (Bijwaard et al., 2001).

To detect genomic loss of the INK4a/ARF, ATM, and p53 tumor suppressor loci in the tumor specimens, we performed quantitative real-time PCR assays using genomic DNA. The REL locus on chromosome 2p was chosen as a reference gene based on comparative genomic hybridization studies that showed only infrequent genomic alterations in this chromosomal region in MCL (Bea et al., 1999; Bentz et al., 2000). Eight control DNA samples were prepared from peripheral blood mononuclear cells of 5 different healthy volunteers. The ratios of INK4a/ARF locus, ATM, and p53 amplification relative to REL amplification were calculated for each control sample. We used these control ratios to establish cutoff ratios that we used to assess tumor DNAs for genomic deletions. For each gene, this cutoff ratio was set as the mean ratio minus 3 standard deviation units; the cutoffs for the INK4a/ARF locus/REL, ATM/REL, and p53/REL ratios were 0.67, 0.72, and 0.7, respectively. A tumor DNA sample that yielded an amplification ratio below the cutoff ratio for a particular tumor suppressor gene was considered to have a genomic deletion of that gene.

We used previously described primer and TaqMan probe sets for the INK4a/ARF locus that were situated in exonic regions that are shared by p16^{INK4a} and p14^{ARF} (Labuhn et al., 2001). The primers used for the REL locus have also been described (Goff et al., 2000). Primers for ATM amplification were 5′-CCCAGACCGCCAATCTCAT (sense) and 5′-ATGGAGTGAGGAGAGGGAGGA (antisense), and for p53, 5′-GGGACCTCTTATCAAGTGGAAA (sense) and 5′-CCCAATTGCAGGTAAAACAGTCA (antisense). Gene-specific fluorescent probes for ATM and p53 were 5′-FAM-CACCCCTCCAGAGTGGCCCTTGA-TAMRA (sense) and 5′-FAM-TTTCCAGTCTAACACTCAAAATGCCGTTTTCTT-TAMRA (sense), respectively.

Statistical methods
Bayesian formulation of a discriminator between two lymphoma subtypes
The method we used to formulate our predictor of MCL was based on a variation of the compound covariate predictor (Radmacher et al., 2002). Although our complete method involved the distinction between MCL and several different classes of samples, we begin by describing a general method for estimating the probability that a given sample is in one of two groups, based on data from a fixed training set.

We begin with a gene selection step. For each gene in our training set, we calculated the t statistic for the difference in the expression of that gene between the two groups. After our data set was so reduced to include only unique genes, we choose the k genes with most statically significant t statistics to use in our predictor. In order to avoid redundancy, when multiple spots for a given gene were found on the array, we only considered the spot that gave the most statistically significant t statistic. This resulted in a list of k unique genes that were variably expressed between the two groups. The method we used to choose k will be discussed later.

Given a training sample, the standard 2-group compound covariate predictor associates with each sample a compound covariate score (CCS) given by

$$CCS(X) = \sum_{j=1}^{k} t_j X_j,$$

where t_j is the t statistic for the two-group comparison of the log ratios for gene j in the training set, and X_j is the log ratio for gene j of the sample. This sum is taken over the k most significant t statistics. This produces a score for which high values indicate likely membership in group 1 and low values indicate likely membership in group 2.

Radmacher et al. suggest classifying a new sample based on whether the CCS of this new sample was closer to the median of the CCSs in each group.

This works well, but does not allow one to make a statement concerning the amount of confidence one has in such an assignment. According to Bayes' rule (Bayes, 1763), we can estimate the probability of a new sample Y being within one of the groups as

$$P(Y \text{ in Group 1} | CCS(Y) =$$

$$\frac{P(CCS(Y)|Y \text{ in Group 1})}{P(CCS(Y)|Y \text{ in Group 1}) + P(CCS(Y)|Y \text{ in Group 2})}.$$

Strictly speaking, there should be additional terms indicating the general prevalence of group 1 and group 2 in the population at large, but since we make no claims as to the representative nature of our patient sample, we eliminated these terms, inherently assuming that Group 1 and Group 2 were equally prevalent.

Since $CCS(X)$ is the linear combination of multiple measurements, it is not unreasonable to assume that the distribution of $CCS(X)$ within each subgroup will be approximately normal. So if we let M_1 and M_2 be the sample means of $CCS(X)$ within group 1 and group 2 of the training set, and s_1^2 and s_2^2 the respected sample variances, we can make the following estimate:

$$P(Y \text{ in Group 1}) =$$

$$\frac{\phi(CCS(Y); M_1, s_1^2)}{\phi(CCS(Y); M_1, s_1^2) + \phi(CCS(Y); M_2, s_2^2)}$$

where ϕ represents the normal density.

$$\phi(x; \mu, \sigma^2) = \frac{1}{\sqrt{2\pi}\sigma} e^{-(x-\mu)/2\sigma^2}.$$

For ease in notation we write

$$P_1(Y) \equiv P(Y \text{ in Group 1}).$$

Formulation of a gene expression-based MCL diagnostic test

We began by equally dividing the gene expression data from MCL and other lymphoma samples into a training set and a validation set. The training set consisted of 46 MCL samples, 42 ABC samples, 67 GCB samples, and 11 SLL samples. The validation set was similarly composed, but had one fewer ABC sample. Since our goal was to determine which genes other than cyclin D1 were related to MCL, we excluded all cyclin D1 clones from this analysis.

In generating an MCL versus non-MCL predictor, a simple two class predictor would be insufficient, since there was a great deal of structure within the non-MCL subset. Instead, we generated 3 separate 2-group predictors: MCL versus ABC, MCL versus GCB, and MCL versus SLL.

Each model was trained only on those elements of the training set that matched the model (i.e., only the MCL and GCB cases were used to train the MCL versus GCB model.) Since a priori the optimal value of k, the number of genes included in a given predictor, was unknown, we used leave-one-out crossvalidation (Hills, 1966) to optimize this value. According to leave-one-out crossvalidation, one sample at a time is removed from the training set, and the remaining samples are used to form a predictor, which is applied to the removed sample. This is repeated each time, reselecting genes and reformulating the predictor, until each sample has been left out once. This method was repeated for different values of k, and we choose the value that gave us the lowest total leave-one-out error probability for a given model. For example for the GCB versus MCL model, we chose the value of k that minimized

$$\sum_{Y \text{ in GCB}} P_{MCL}(Y) + \sum_{Y \text{ in MCL}} P_{GCB}(Y)$$

Where the probabilities are computed based on a training set of all samples except Y. This optimization resulted in $k = 9$ for the GCB versus MCL predictor, $k = 20$ genes for ABC versus MCL predictor, and $k = 85$ for the SLL versus MCL predictor.

Using these k values, we now used the entire training set to generate the three predictors and applied it to the training set. We defined a patient, Y, as MCL only if $P_{MCL}(Y) > 0.9$ for all three predictors. This resulted in only one misclassification, in which an MCL predictor had $P_{ABC}(Y) > 0.9$. Incidentally, we also observed that all of the non-MCL patients were correctly assigned by their respective predictors with p > 0.9. (i.e., $P_{GCB}[Y] > 0.9$ for all Y in GCB on the validation set, etc.).

Other statistical methods

Survival curves and median survival times were estimated using the Kaplan-Meier method. When estimating the association of parameters with survival, Cox proportional hazards models were fit. For continuous variables, (proliferation and cyclin D1 coding region expression), the likelihood ratio p value was reported. For the categorical variables (tumor histology, high/low cyclin D1 3′ UTR, INK4a/ARF deletion, p53 deletion, and ATM deletion), the p value from the log rank test was used. A Cox model was also fit to the combination of the cyclin D1 coding region expression and an indicator of INK4a/ARF deletion. For the purpose of displaying survival curves in Figure 5C, the samples were ranked according to this model and divided into quartiles. A likelihood ratio p value was reported from the combined model.

A Spearman rank correlation test was used to indicate the association between proliferation and expression of the cyclin D1 coding region. When determining differences between the high/low cyclin D1 3′ UTR in proliferation and cyclin D1 coding region expression, the p value from a 2-sided t test was reported. t tests were also used to determine the extent to which genes were differentially expressed between MCL and each other lymphoma subtypes. An ANOVA model was used to determine the extent to which INK4a/ARF locus deletion and cyclin D1 coding region expression added constructively in their association with proliferation.

In forming the predictor of survival, we used those genes that were found in the proliferation signature, were associated with poor prognosis in the training set (p < 0.001 according to a Wald test), and had larger variance across the samples of the training set than 2/3 of the genes. When multiple Lymphochip microarray features representing the same gene were found to satisfy these conditions, only the feature that was most significantly associated with survival on the training set was used. No survival information from the validation set was used to generate the gene list. The expression data for each of these genes were mean centered across all samples, and the proliferation signature average for a given sample was computed as the average of these mean centered observations. Missing values for genes were excluded in taking this average.

References

Alizadeh, A., Eisen, M., Davis, R.E., Ma, C., Sabet, H., Tran, T., Powell, J., Yang, L., Marti, G., Moore, T., et al. (1999). The Lymphochip: A specialized cDNA microarray for the genomic-scale analysis of gene expression in normal and malignant lymphocytes. Cold Spring Harb. Symp. Quant. Biol. *64*, 71–78.

Argatoff, L.H., Connors, J.M., Klasa, R.J., Horsman, D.E., and Gascoyne, R.D. (1997). Mantle cell lymphoma: a clinicopathologic study of 80 cases. Blood *89*, 2067–2078.

Barista, I., Romaguera, J.E., and Cabanillas, F. (2001). Mantle-cell lymphoma. Lancet Oncol *2*, 141–148.

Bayes, T. (1763). An essay towards solving a problem in the doctrine of chances. Phil Trans Roy Soc London *53*, 370.

Bea, S., Ribas, M., Hernandez, J.M., Bosch, F., Pinyol, M., Hernandez, L., Garcia, J.L., Flores, T., Gonzalez, M., Lopez-Guillermo, A., et al. (1999). Increased number of chromosomal imbalances and high-level DNA amplifications in mantle cell lymphoma are associated with blastoid variants. Blood *93*, 4365–4374.

Bea, S., Tort, F., Pinyol, M., Puig, X., Hernandez, L., Hernandez, S., Fernandez, P.L., van Lohuizen, M., Colomer, D., and Campo, E. (2001). BMI-1 gene amplification and overexpression in hematological malignancies occur mainly in mantle cell lymphomas. Cancer Res. *61*, 2409–2412.

Bentz, M., Plesch, A., Bullinger, L., Stilgenbauer, S., Ott, G., Muller-Hermelink, H.K., Baudis, M., Barth, T.F., Moller, P., Lichter, P., and Dohner, H.

(2000). t(11;14)-positive mantle cell lymphomas exhibit complex karyotypes and share similarities with B-cell chronic lymphocytic leukemia. Genes Chromosomes Cancer 27, 285–294.

Bijwaard, K.E., Aguilera, N.S., Monczak, Y., Trudel, M., Taubenberger, J.K., and Lichy, J.H. (2001). Quantitative real-time reverse transcription-PCR assay for cyclin D1 expression: utility in the diagnosis of mantle cell lymphoma. Clin. Chem. 47, 195–201.

Bosch, F., Jares, P., Campo, E., Lopez-Guillermo, A., Piris, M.A., Villamor, N., Tassies, D., Jaffe, E.S., Montserrat, E., Rozman, C., et al. (1994). PRAD-1/cyclin D1 gene overexpression in chronic lymphoproliferative disorders: a highly specific marker of mantle cell lymphoma. Blood 84, 2726–2732.

Bosch, F., Lopez-Guillermo, A., Campo, E., Ribera, J.M., Conde, E., Piris, M.A., Vallespi, T., Woessner, S., and Montserrat, E. (1998). Mantle cell lymphoma: presenting features, response to therapy, and prognostic factors. Cancer 82, 567–575.

Campo, E., Raffeld, M., and Jaffe, E.S. (1999). Mantle-cell lymphoma. Semin. Hematol. 36, 115–127.

de Boer, C.J., van Krieken, J.H., Kluin-Nelemans, H.C., Kluin, P.M., and Schuuring, E. (1995). Cyclin D1 messenger RNA overexpression as a marker for mantle cell lymphoma. Oncogene 10, 1833–1840.

Dreyling, M.H., Bullinger, L., Ott, G., Stilgenbauer, S., Muller-Hermelink, H.K., Bentz, M., Hiddemann, W., and Dohner, H. (1997). Alterations of the cyclin D1/p16-pRB pathway in mantle cell lymphoma. Cancer Res. 57, 4608–4614.

Eischen, C.M., Weber, J.D., Roussel, M.F., Sherr, C.J., and Cleveland, J.L. (1999). Disruption of the ARF-Mdm2-p53 tumor suppressor pathway in Myc-induced lymphomagenesis. Genes Dev. 13, 2658–2669.

Goff, L.K., Neat, M.J., Crawley, C.R., Jones, L., Jones, E., Lister, T.A., and Gupta, R.K. (2000). The use of real-time quantitative polymerase chain reaction and comparative genomic hybridization to identify amplification of the REL gene in follicular lymphoma. Br. J. Haematol. 111, 618–625.

Gopal, A.K., Rajendran, J.G., Petersdorf, S.H., Maloney, D.G., Eary, J.F., Wood, B.L., Gooley, T.A., Bush, S.A., Durack, L.D., Martin, P.J., et al. (2002). High-dose chemo-radioimmunotherapy with autologous stem cell support for relapsed mantle cell lymphoma. Blood 99, 3158–3162.

Greiner, T.C., Moynihan, M.J., Chan, W.C., Lytle, D.M., Pedersen, A., Anderson, J.R., and Weisenburger, D.D. (1996). p53 mutations in mantle cell lymphoma are associated with variant cytology and predict a poor prognosis. Blood 87, 4302–4310.

Hernandez, L., Fest, T., Cazorla, M., Teruya-Feldstein, J., Bosch, F., Peinado, M.A., Piris, M.A., Montserrat, E., Cardesa, A., Jaffe, E.S., et al. (1996). p53 gene mutations and protein overexpression are associated with aggressive variants of mantle cell lymphomas. Blood 87, 3351–3359.

Hills, M. (1966). Allocation rules and error rates. J. Royal. Statis. Soc. B 28, 1–31.

Jacobs, J.J., Kieboom, K., Marino, S., DePinho, R.A., and van Lohuizen, M. (1999). The oncogene and Polycomb-group gene bmi-1 regulates cell proliferation and senescence through the ink4a locus. Nature 397, 164–168.

Jaffe, E.S., Harris, N.L., Diebold, J., and Muller-Hermelink, H.K. (1999). World Health Organization classification of neoplastic diseases of the hematopoietic and lymphoid tissues. A progress report. Am. J. Clin. Pathol. 111, S8–S12.

Jaffe, E.S., Harris, N.L., Stein, H., and Vardiman, J.W. (2001). Tumours of Haematopoietic and Lymphoid Tissues (Lyon, IARC Press).

Kamijo, T., Zindy, F., Roussel, M.F., Quelle, D.E., Downing, J.R., Ashmun, R.A., Grosveld, G., and Sherr, C.J. (1997). Tumor suppression at the mouse INK4a locus mediated by the alternative reading frame product p19ARF. Cell 91, 649–659.

Kamijo, T., Weber, J.D., Zambetti, G., Zindy, F., Roussel, M.F., and Sherr, C.J. (1998). Functional and physical interactions of the ARF tumor suppressor with p53 and Mdm2. Proc. Natl. Acad. Sci. USA 95, 8292–8297.

Karlseder, J., Broccoli, D., Dai, Y., Hardy, S., and de Lange, T. (1999). p53- and ATM-dependent apoptosis induced by telomeres lacking TRF2. Science 283, 1321–1325.

Kastan, M.B., Zhan, Q., el-Deiry, W.S., Carrier, F., Jacks, T., Walsh, W.V., Plunkett, B.S., Vogelstein, B., and Fornace, A.J., Jr. (1992). A mammalian cell cycle checkpoint pathway utilizing p53 and GADD45 is defective in ataxia-telangiectasia. Cell 71, 587–597.

Labuhn, M., Jones, G., Speel, E.J., Maier, D., Zweifel, C., Gratzl, O., Van Meir, E.G., Hegi, M.E., and Merlo, A. (2001). Quantitative real-time PCR does not show selective targeting of p14(ARF) but concomitant inactivation of both p16(INK4A) and p14(ARF) in 105 human primary gliomas. Oncogene 20, 1103–1109.

Lardelli, P., Bookman, M.A., Sundeen, J., Longo, D.L., and Jaffe, E.S. (1990). Lymphocytic lymphoma of intermediate differentiation. Morphologic and immunophenotypic spectrum and clinical correlations. Am. J. Surg. Pathol. 14, 752–763.

Lebwohl, D.E., Muise-Helmericks, R., Sepp-Lorenzino, L., Serve, S., Timaul, M., Bol, R., Borgen, P., and Rosen, N. (1994). A truncated cyclin D1 gene encodes a stable mRNA in a human breast cancer cell line. Oncogene 9, 1925–1929.

Leonard, J.P., Schattner, E.J., and Coleman, M. (2001). Biology and management of mantle cell lymphoma. Curr. Opin. Oncol. 13, 342–347.

Lin, S., Wang, W., Wilson, G.M., Yang, X., Brewer, G., Holbrook, N.J., and Gorospe, M. (2000). Down-regulation of cyclin D1 expression by prostaglandin A(2) is mediated by enhanced cyclin D1 mRNA turnover. Mol. Cell. Biol. 20, 7903–7913.

Louie, D.C., Offit, K., Jaslow, R., Parsa, N.Z., Murty, V.V., Schluger, A., and Chaganti, R.S. (1995). p53 overexpression as a marker of poor prognosis in mantle cell lymphomas with t(11;14)(q13;q32). Blood 86, 2892–2899.

Perkins, E.J., Nair, A., Cowley, D.O., Van Dyke, T., Chang, Y., and Ramsden, D.A. (2002). Sensing of intermediates in V(D)J recombination by ATM. Genes Dev. 16, 159–164.

Pinyol, M., Hernandez, L., Cazorla, M., Balbin, M., Jares, P., Fernandez, P.L., Montserrat, E., Cardesa, A., Lopez-Otin, C., and Campo, E. (1997). Deletions and loss of expression of p16INK4a and p21Waf1 genes are associated with aggressive variants of mantle cell lymphomas. Blood 89, 272–280.

Pinyol, M., Cobo, F., Bea, S., Jares, P., Nayach, I., Fernandez, P.L., Montserrat, E., Cardesa, A., and Campo, E. (1998). p16(INK4a) gene inactivation by deletions, mutations, and hypermethylation is associated with transformed and aggressive variants of non-Hodgkin's lymphomas. Blood 91, 2977–2984.

Pinyol, M., Hernandez, L., Martinez, A., Cobo, F., Hernandez, S., Bea, S., Lopez-Guillermo, A., Nayach, I., Palacin, A., Nadal, A., et al. (2000). INK4a/ARF locus alterations in human non-Hodgkin's lymphomas mainly occur in tumors with wild-type p53 gene. Am. J. Pathol. 156, 1987–1996.

Quintanilla-Martinez, L., Davies-Hill, T., Fend, F., Calzada-Wack, J., Sorbara, L., Campo, E., Jaffe, E.S., and Raffeld, M. (2003). Sequestration of p27kip1 protein by cyclin D1 in typical and blastic variants of mantle cell lymphomas (MCL): implication for pathogenesis. Blood, in press.

Radmacher, M.D., McShane, L.M., and Simon, R. (2002). A paradigm for class prediction using gene expression profiles. J. Comput. Biol. 9, 505–511.

Raffeld, M., and Jaffe, E.S. (1991). bcl-1, t(11;14), and mantle cell-derived lymphomas. Blood 78, 259–263.

Randle, D.H., Zindy, F., Sherr, C.J., and Roussel, M.F. (2001). Differential effects of p19(Arf) and p16(Ink4a) loss on senescence of murine bone marrow-derived preB cells and macrophages. Proc. Natl. Acad. Sci. USA 98, 9654–9659.

Raty, R., Franssila, K., Joensuu, H., Teerenhovi, L., and Elonen, E. (2002). Ki-67 expression level, histological subtype, and the International Prognostic Index as outcome predictors in mantle cell lymphoma. Eur. J. Haematol. 69, 11–20.

Rimokh, R., Berger, F., Bastard, C., Klein, B., French, M., Archimbaud, E., Rouault, J.P., Santa Lucia, B., Duret, L., Vuillaume, M., et al. (1994). Rearrangement of CCND1 (BCL1/PRAD1) 3′ untranslated region in mantle-cell lymphomas and t(11q13)-associated leukemias. Blood 83, 3689–3696.

Rosenberg, C.L., Wong, E., Petty, E.M., Bale, A.E., Tsujimoto, Y., Harris, N.L., and Arnold, A. (1991). PRAD1, a candidate BCL1 oncogene: mapping

and expression in centrocytic lymphoma. Proc. Natl. Acad. Sci. USA *88*, 9638–9642.

Rosenwald, A., Wright, G., Chan, W.C., Connors, J.M., Campo, E., Fisher, R.I., Gascoyne, R.D., Muller-Hermelink, H.K., Smeland, E.B., Giltnane, J.M., et al. (2002). The use of molecular profiling to predict survival after chemotherapy for diffuse large-B-cell lymphoma. N. Engl. J. Med. *346*, 1937–1947.

Schmitt, C.A., Fridman, J.S., Yang, M., Lee, S., Baranov, E., Hoffman, R.M., and Lowe, S.W. (2002). A senescence program controlled by p53 and p16INK4a contributes to the outcome of cancer therapy. Cell *109*, 335–346.

Seto, M., Yamamoto, K., Iida, S., Akao, Y., Utsumi, K.R., Kubonishi, I., Miyoshi, I., Ohtsuki, T., Yawata, Y., Namba, M., et al. (1992). Gene rearrangement and overexpression of PRAD1 in lymphoid malignancy with t(11;14)(q13;q32) translocation. Oncogene *7*, 1401–1406.

Shaffer, A.L., Rosenwald, A., Hurt, E.M., Giltnane, J.M., Lam, L.T., Pickeral, O.K., and Staudt, L.M. (2001). Signatures of the immune response. Immunity *15*, 375–385.

Sherr, C.J., and McCormick, F. (2002). The RB and p53 pathways in cancer. Cancer Cell *2*, 103–112.

Sherr, C.J., and Roberts, J.M. (1995). Inhibitors of mammalian G1 cyclin-dependent kinases. Genes Dev. *9*, 1149–1163.

Sherr, C.J., and Roberts, J.M. (1999). CDK inhibitors: positive and negative regulators of G1-phase progression. Genes Dev. *13*, 1501–1512.

Swerdlow, S.H., and Williams, M.E. (2002). From centrocytic to mantle cell lymphoma: a clinicopathologic and molecular review of 3 decades. Hum. Pathol. *33*, 7–20.

TNHLCP (The Non-Hodgkin's Lymphoma Classification Project.) (1997). A clinical evaluation of the International Lymphoma Study Group classification of non-Hodgkin's lymphoma. Blood *89*, 3909–3918.

Velders, G.A., Kluin-Nelemans, J.C., De Boer, C.J., Hermans, J., Noordijk, E.M., Schuuring, E., Kramer, M.H., Van Deijk, W.A., Rahder, J.B., Kluin, P.M., and Van Krieken, J.H. (1996). Mantle-cell lymphoma: a population-based clinical study. J. Clin. Oncol. *14*, 1269–1274.

Weisenburger, D.D., and Armitage, J.O. (1996). Mantle cell lymphoma–an entity comes of age. Blood *87*, 4483–4494.

Withers, D.A., Harvey, R.C., Faust, J.B., Melnyk, O., Carey, K., and Meeker, T.C. (1991). Characterization of a candidate bcl-1 gene. Mol. Cell. Biol. *11*, 4846–4853.

Xiong, Y., Connolly, T., Futcher, B., and Beach, D. (1991). Human D-type cyclin. Cell *65*, 691–699.

Yatabe, Y., Suzuki, R., Tobinai, K., Matsuno, Y., Ichinohasama, R., Okamoto, M., Yamaguchi, M., Tamaru, J., Uike, N., Hashimoto, Y., et al. (2000). Significance of cyclin D1 overexpression for the diagnosis of mantle cell lymphoma: a clinicopathologic comparison of cyclin D1-positive MCL and cyclin D1-negative MCL-like B-cell lymphoma. Blood *95*, 2253–2261.